International Symposium
On Turbulence and Shear Flow
Phenomena (TSFP-9)
June 30 - July 3, 2015 *Melbourne, Australia*



# COMPARISON OF DIFFERENT LES-BASED COMBUSTION MODELS APPLIED TO A REACTING N-HEPTANE SPRAY

**Fernando Luiz Sacomano Filho**
Institute for Energy and Power Plant Technology
Technische Universität Darmstadt
Jovanka-Bontschits-Strasse 2, 64287 Darmstadt, Germany
sacomano@ekt.tu-darmstadt.de

**Mouldi Chrigui**
Institute for Energy and Power Plant Technology / U. R. Materiaux, Energie et Energies Renouvelales
Technische Universität Darmstadt / Université de Gafsa
Jovanka-Bontschits-Strasse 2, 64287 Darmstadt, Germany / C. U. Sidi Ahmed Zarroug Gafsa 2112
mchrigui@ekt.tu-darmstadt.de

**Amsini Sadiki**
Institute for Energy and Power Plant Technology
Technische Universität Darmstadt
Jovanka-Bontschits-Strasse 2, 64287 Darmstadt, Germany
mchrigui@ekt.tu-darmstadt.de

## ABSTRACT

The prediction performance of turbulent spray flames with two sub-grid scale combustion models, namely the presumed Probability Density Function (PDF) approach and the Artificially Thickened Flame (ATF) model, is evaluated for Large Eddy Simulations (LES) in an Eulerian-Lagrangian framework. To include detailed chemistry effects without solving all species transport equations the Flamelet Generated Manifold (FGM) method is adopted. Quantitative comparisons between both models achievements are provided for spray and flame properties using available experimental data. The spray properties include characteristic droplet diameters, mean axial velocity and its fluctuations, while a reaction progress variable is available for the flame structure. It turns out that both models are able to predict the increase of the flame length as leaner became the mixture as well as the spray characteristics at the investigated positions. However, the predictions obtained with the ATF model agree most favorably with experimental measurements.

## INTRODUCTION

Spray combustion may feature the simultaneous presence of gaseous single phase flame modes, namely premixed and non premixed combustion.The coexistence of these modes is a feasible output originated by the combination of droplets evaporation and the structure of flow fields (Reveillon & Vervisch (2005)). As the modeling approaches derived for turbulent combustion are often based on the previous classification of the reaction processes (Poinsot & Veynante (2012)), the existence of multiple flame types in a reacting two-phase flow requires more care on the definition of the computational methods.

Attention has been given in the statistical description of the turbulence-spray-flame interaction along with the usage of probability density functions (PDF) (Jenny *et al.* (2012); Knudsen & Pitsch (2015); Ge & Gutheil (2008); Jones *et al.* (2015); Prasad *et al.* (2013)). The transported PDF fields (Jones *et al.* (2015); Prasad *et al.* (2013)) shown to be a promising tool for the prediction of spray flames, since it can recover the singularities of spray PDFs (Ge & Gutheil (2008)) and is also able to consider the simultaneousness of different flame modes. However, the higher number of fields required to recover the correct PDF profiles as well the necessity of detailed chemistry to reproduce the reaction rate make it prohibitive to Large Eddy Simulations (LES) of practical systems. An alternative to handle the multiple combustion regimes using tabulated chemistry is presented by Knudsen & Pitsch (2015), who utilized two look-up tables (originated from premixed and non premixed flamelets, respectively), to compute turbulent swirling flames. To account for the statistical treatment of the turbulence-flame interactions, they adopted a presumed PDF approach based on $\beta$ distribution functions. Presumed PDF approaches, despite of being shown by Ge & Gutheil (2008) that are not able to reproduce the bi-modality of the PDFs encountered in spray flames, are still usual methods to compute turbulent spray flames (Chrigui *et al.* (2012); Sacomano Filho *et al.* (2014); Chrigui *et al.* (2013); Knudsen & Pitsch (2015)).

Recently, Boileau *et al.* (2008*a*) and Boileau *et al.* (2008*b*) showed the great capability of the Artificially Thickened Flame (ATF) method on predicting the behavior of turbulent spray flames based on Eulerian-Eulerian

framework and one-step irreversible chemistry. This modeling technique, formerly developed to compute laminar premixed flames (O'Rourke & Bracco (1979)) was gradually adapted to compute turbulent premixed flames (Charlette *et al.* (2002); Colin *et al.* (2000)) and stratified flames (Kuenne *et al.* (2012)).

In order to assess the influence of the combustion modeling on the computation of turbulent spray combustion, the usual presumed PDF approach based on $\beta$ distribution functions is compared with the recently exploited ATF method. Despite of the different combustion models, the same chemical database is adopted. Both techniques use the Flamelet Generated Manifold (FGM) method to reduce the 88 species and 387 intermediary reactions available in the mechanism proposed by Yoo *et al.* (2011) to represent the n-heptane combustion. The unsteadiness arising from the turbulent dispersion of evaporating droplets are captured by an Eulerian-Lagrangian spray module relying on the LES method. An evaporation model accounting for the interphase non equilibrium is applied to describe the droplet evaporation process. Concerning the better conditioning of the reaction process and avoiding the appearance of markable simultaneous flame modes, two of the Lean Partially Pre-vaporized (LPP) flames investigated experimentally in Pichard (2003) are selected to guide the addressed discussions.

## MODELING APPROACHES

An Eulerian-Lagrangian approach is adopted to represent the two-phase flow in this work. This approach describes the gas phase as a continuous media in an Eulerian framework, whereas the liquid phase is composed by a set of disperse droplets followed in a Lagrangian specification. Although, in this context, both phases are treated separately, a full inter-phase two-way coupling is done. The carrier gas phase quantities are interpolated in droplets positions, while the perturbations originated by the disperse phase are introduced through source terms in the computational cells. As a result, both phases are treated in a non conservative form.

### Gas Phase

The turbulent motions of the carrier phase are described in the Large Eddy Simulations (LES) context following a variable-density low Mach number formulation. In the Flamelet Generated Manifold (FGM) framework, the chemistry is recovered by two control variables, namely the mixture fraction ($z$) and the reaction progress variable ($Y_{RPV}$). While the mass and momentum equations are described according to Chrigui *et al.* (2012), the general transport equation of any control variable, $\psi$, is given by Eq. 1.

$$\frac{\partial(\overline{\rho}\tilde{\psi})}{\partial t}+\frac{\partial(\overline{\rho}\tilde{\psi}\widetilde{u_j})}{\partial x_j}=\frac{\partial}{\partial x_j}\left[\left(FE\frac{\overline{\mu}}{Sc_\psi}-\overline{\rho}(1-\Omega)\frac{\mu_t}{Sc_{t,\psi}}\right)\frac{\partial\tilde{\psi}}{\partial x_j}\right]+\frac{E}{F}\widetilde{\dot{\omega}_\psi}+\frac{\overline{S_{\psi,v}}}{F} \quad (1)$$

The filtered variables are obtained from spatial filtering as $\psi=\tilde{\psi}+\psi''$ with $\tilde{\psi}=\overline{\rho\psi}/\overline{\rho}$. Over-bars and tildes express spatially filtered and density-weighted filtered values with a filter width $\Delta_{mesh}$, respectively, while double prime represents sub-grid scale (SGS) fluctuations. $\rho$ is the mixture density, $t$ time, $u_j$ the components of velocity in $i$ ($i=1,2,3$) direction, $x_j$ Cartesian coordinate in $j$ direction and $\mu$ the dynamic viscosity. The quantity $F$ corresponds to the thickening factor, $E$ to the efficiency function, $\Omega$ is the flame sensor and $Sc$ the Schmidt number. Details about these last four quantities are addressed in the combustion modeling description.

The source term $\dot{\omega}_\psi$ corresponds to the reaction rate for the $Y_{RPV}$ transport equation and is set to zero for the $z$ equation. $\overline{S_{\psi,v}}$ refers to source of evaporated fuel from the disperse phase, which is responsible to modify the mixture quality [1]. This source term is included in the $z$ transport equation, however, since fuel is not incorporated in the reaction progress variable used in this work (see combustion modeling section), no source of vapor is present in $Y_{RPV}$ balance equation. More description about how this source terms are computed can be found in Sacomano Filho *et al.* (2014).

### Disperse Phase

A brief description of the discrete phase modeling is delivered in this section. For more details the reader is referred to Sacomano Filho *et al.* (2014).

The computation of the droplet motion considers only drag and buoyancy forces. Regarding that the density ratio of liquid n-heptane and the gaseous mixture has an order of $10^3$, complementary forces can be neglected. Hence, the parcel velocity can be achieved by the integration of Eq. 2.

$$\frac{du_{p,i}}{dt}=\frac{3}{4}\frac{C_D}{d_p}\frac{\rho}{\rho_p}|\vec{u}-\vec{u_p}|(u_i-u_{p,i})+\frac{(\rho_p-\rho)}{\rho_p}g_i \quad (2)$$

where, the drag coefficient, $C_D$, is computed similarly as done in Chrigui *et al.* (2013). $g_i$ is the gravitational acceleration in $i$ ($i=1,2,3$) direction and subscripts $\psi_p$ are associated with droplets quantities. Attention shall be given in Eq. 2 to the fact that velocities are expressed by instantaneous values. To obtain these values from the filtered transported quantities, SGS fluctuations should be considered along with a dispersion model. However, despite the importance of the SGS dispersion modeling, for the sake of simplification, no SGS fluctuations are accounted for in this work. we rather rely on the fact that in our LES at least 80% of the turbulence energy of the carrier phase is captured, so that the dispersion is partially considered.

To describe the evaporation process, the infinite liquid conductivity approach for the non equilibrium evaporation model of Bellan & Harstad (1987) following the formulation of Miller *et al.* (1998) is applied. Since droplets carried by the gas phase have diameter smaller than 50 $\mu$m, the uniform temperature assumption is reasonable.

### Combustion Modeling

In LES context the filtered large scales of the mixture composition field are solved. However, observing that the thickness of reaction zones is usually one order of magnitude lower than a typical LES mesh cell, a sub-grid scale modeling must be considered. In the investigations performed here, two combustion models are used to recover the

[1] The thickening of the source term $\overline{S_{\psi,v}}$ can be omitted in the Eulerian phase calculation so long its counterpart in the Lagrangian phase is also omitted. This option avoids a mass unbalance in the computational procedure and generates the same effect of the thickening in both sides without extra processing efforts.

turbulence-flame interaction: presumed PDF, Artificially Thickened Flame. Both methods are described in the following.

**Presumed PDF approach** One of the forms to represent the turbulence-flame interaction is based on stochastic methods. In these methods, statistical distributions of the control variables are used to describe the fluctuating values of their related quantities. Accordingly, these distributions can be computed on-line, during the simulation course, under high computational costs or can be simply predefined through a shape function, i.e. a presumed PDF.

When the presumed PDF approach is coupled with the FGM method, the chemical database can be previously integrated over the joint PDF of the control variables resulting in a look-up table. In the present work the statistical independence between $z$ and $Y_{RPV}$ is assumed. As a consequence, the joint PDF is written as the product between the PDFs of these two control variables, which are described by $\beta$ shape functions.

The integrated look-up table has a dimension of 4 (901x101x11x5), spanned by its four entries: $\widetilde{z}$, $\widetilde{Y_{RPV}}$, $\widetilde{z''^2}$ and $\widetilde{Y_{RPV}''^2}$. To compute control variables variances ($\widetilde{z''^2}$ and $\widetilde{Y_{RPV}''^2}$), a gradient-based model (Eq. 3) similar to that used in (Vreman *et al.* (2008); Chrigui *et al.* (2012); Sacomano Filho *et al.* (2014)) is adopted as a first-approach.

$$\widetilde{\psi''^2} = C_{eq}\Delta^2_{mesh}\left(\frac{\partial\widetilde{\psi}}{\partial x_j}\right)^2 \tag{3}$$

where the parameter $C_{eq}$ has a value of 0.1.

As already mentioned in the carrier phase modeling description, Eq. 1 is used to transport the control variables for both combustion models. However, in the $\beta$-PDF approach the thickening factor, efficiency function and flame sensor are set to constant values, such as: $F = 1$, $E = 1$ and $\Omega = 0$; since they are exclusive variables of the ATF model.

**ATF method** The main feature of the ATF is to allow the reaction zone to be solved in a mesh with typical LES/RANS (Reynolds Averaged Navier-Stokes) cell size. This characteristic is quite attractive to model propagating flames, so that the reaction properties can be directly recovered from the chemical kinetics. The thickening of the reaction zone is obtained through a coordinate transformation of the scalar transport equations, relying on their mathematical invariance. Accordingly, the length-scales and time-scales of the scalar fields are increased by the thickening factor (Vreman *et al.* (2008)).

Observing that the scales of the scalar fields are modified, whereas no changes are done in the momentum and continuity equations, the interaction of the chemistry with the turbulence is affected by the artificial thickening. To overcome this problem, Meneveau & Poinsot (1991) proposed the introduction of an efficiency function ($E$) in the modified balance equations. In this way, the loss of flame surface caused by thickening is corrected by means of the SGS turbulent flame speed.

In our simulations, the efficiency function derived by Charlette *et al.* (2002) is selected due to its broad applicability. Furthermore, it is important to highlight that in FGM

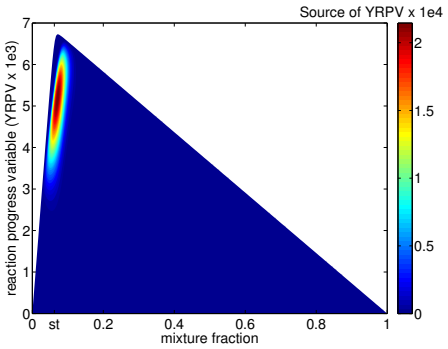


Figure 1. Illustration of the FGM database: $Y_{RPV}$ vs. $z$ colored by $\dot{\omega}_{RPV}$

context just the transport equations of the control variables undergo the process of thickening.

Considering that the evaporation of droplets is directly dependent on the mixture composition, its correct prediction is extremely important for spray combustion simulation. Therefore, to ensure an accurate computation of the pure mixing, the thickening procedure is performed when the flame is detected by the flame sensor derived by Durand & Polifke (2007), described by Eq. 4.

$$\Omega = 16[c(1-c)]^2, \quad c = Y_{RPV}/Y^{eq}_{RPV} \tag{4}$$

where $Y^{eq}_{RPV}$ is the maximum value of $Y_{RPV}$ for a specific mixture composition. Following this procedure, $F$ is dynamically computed by:

$$F = 1 + (F_{max} - 1)\Omega, \quad F_{max} = max(1, \Delta_{mesh}/\Delta_{x,max}) \tag{5}$$

in which $F_{max}$ is defined according to the cell size ($\Delta_{mesh}$) and the maximum cell size necessary to capture the laminar flame speed with less than 10 % error in one-dimensional simulations ($\Delta_{x,max}$) (Kuenne *et al.* (2012)).

It is worthy to notice that, in the ATF approach, the variance of the control variables is not computed, since the reaction zone is solved in the current grid under the flamelet hypothesis and the remaining SGS wrinkling is modeled by $E$. Thus, only two entries ($\widetilde{z}$ and $\widetilde{Y_{RPV}}$) are necessary to access the look-up table for ATF computations.

## Chemistry

To construct the FGM database, flamelets are generated through the computation of one-dimensional adiabatic free propagating flames (premixed) at constant equivalence ratio ($\phi$) with the code CHEM1D (Oijen (2015)). These flamelets are computed for a band of $\phi$ defined between the flammability limits. Outside these limits, interpolations are performed to define the manifold over the whole range of the mixture fraction [0,1]. The temperature set for the CHEM1D simulations is 303K, which corresponds to the initial air temperature of the investigated experimental configuration. The resulting FGM table is depicted in Fig. 1.

The validity of the table was checked by comparing the results of laminar flame speeds computed with the code FASTEST3D and with detailed chemistry calculations done with the code CHEM1D, as shown in Fig. 2.

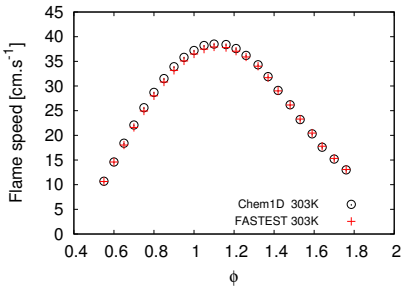


Figure 2. Verification of the FGM database: Comparison of the laminar flame speed achieved with detailed chemistry (CHEM1D) and with FGM (FASTEST)

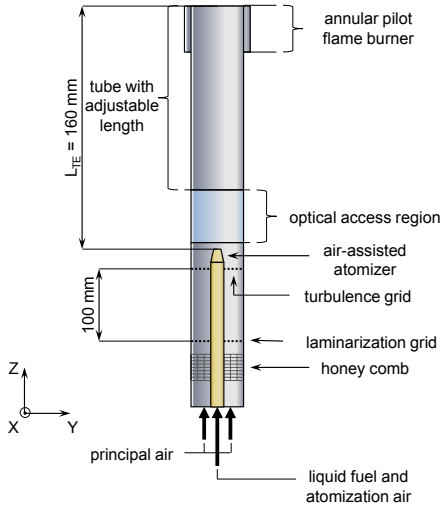


Figure 3. Scheme of the CNRS-Órleans burner (Pichard (2003)).

The composition of $Y_{RPV}$ used in our analysis is given by Eq. 6. The choice of the chemical species as well as the weight factors was done in order to guarantee the monotonicity of this quantity for the whole range of the mixture fraction.

$$Y_{RPV} = \frac{Y_{CO_2}}{Mw_{CO_2}} + \frac{Y_{H_2O}}{2Mw_{H_2O}} + \frac{Y_{CO}}{2Mw_{CO}} \qquad (6)$$

## CONFIGURATION AND NUMERICAL SETUP

For a better conditioning of the reaction process and in order to avoid the appearance of simultaneous flame modes the configuration of Pichard (2003) is chosen. This is one of the spray flame databases listed by Jenny *et al.* (2012) and accepted as one of the target flames at the International Workshop on Turbulent Spray Combustion (TCS).

As illustrated in Fig. 3, the configuration provides a spray jet flame of n-heptane stabilized by a pilot flame. The spray jet is produced by an air-assisted atomizer evolved by a co-flow of air (principal air) under controlled temperature conditions. In this sense, before the flow reaches the flame zone, droplets traverse a pre-vaporization distance and release part of their mass. As a consequence, this feature gives the LPP characteristic to this burner.

In the present simulations, atomization and dense spray zone are not included. Focused on the diluted spray region, the boundary conditions for the disperse phase are set at 85 mm downstream the atomizer's tip, where experimental data are available. Two flames are investigated in this work, which differentiate between each other by the amount of injected liquid fuel (0.094 g/s and 0.104 g/s), which is reflected in the global equivalence ratio, $\phi_g$ (0.79 and 0.87, respectively). The mass flux of atomization air is 0.115 g/s, while that of principal air is 1.69 g/s.

The computations are performed with the coupled version of the academic software FASTEST3D, in which the Lagrangian subroutines are integrated into the Eulerian solver. Two meshes are used in this work to analyze the grid influence on the results. The coarser grid amounts 1,570,480 cells and the finer is defined by 2,983,257 control volumes. Since no considerable difference was observed comparing the results obtained with both grids with the ATF method, the coarser is adopted in our analysis.

The disperse phase boundary conditions are derived from experimental data, whereas droplets size distributions are extracted from measured profiles of the number of droplets, $D_{10}$, $D_{20}$ and $D_{30}$ assuming log-normal distributions. One parcel per class (total 287 classes) is injected within a coupling step ($\Delta t = 1.2 \cdot 10^{-5} \Rightarrow CFL \sim 0.75$). This amounts circa $10^6$ tracked parcels in the flow field.

## RESULTS AND DISCUSSION

Comparisons of simulations results with experimental data are used to validate the proposed modeling approaches. Fig. 4 shows the comparison of radial profiles of characteristic droplets diameters ($D_{pq} = [\sum_k d_k^p N_k / \sum_k d_k^q N_k]^{1/(p-q)}$, $d_k$ is the diameter of the $k^{th}$ parcel) for the flame with $\phi_g = 0.79$ at two axial positions from the burner exit: $0.2Z/D$ and $0.5Z/D$ ($D$ is the inner diameter of the burner exit). This comparison shows that the modeling approach is able to capture correctly the droplets size distributions in the flame zone. Furthermore, it can be observed that these distributions are quite homogeneous along the radial direction.

Good agreement is also observed for the radial profiles of droplets mean axial velocity and its fluctuations at $0.2Z/D$ and $0.5Z/D$ from the burner exit for the flame with $\phi_g = 0.79$ (see Fig. 5). These results together with the droplets size predictions shown that the dispersion of droplets promoted by LES is acceptable in the current simulations.

Regarding the importance of the evaporation process on the mixture preparation and consequently on the flame structure, the evaporation degree ($\theta$) for both flames and both combustion models is plotted in Fig. 6. The quantity $\theta$ can be written as:

$$\theta = (\dot{m}_g - \dot{m}_l(Z)/\dot{m}_g) \qquad (7)$$

where, $\dot{m}_l$ refers to the liquid mass flux in a cross section of the burner locate at a distance ($Z$) from the atomizer exit and $\dot{m}_g$ refers to the total injected mass of liquid fuel.

The structure of the four simulated flames is depicted in Fig. 7, where the instantaneous fields of $z$ show the strong mixture stratifications originated by droplets evaporation. Experimental data of the progress variable defined in Pichard *et al.* (2002) are also included for the flames with $\phi_g = 0.87$ [2]. From this picture the effects of the combustion

[2]The available data is extracted for a air temperature of 298K.

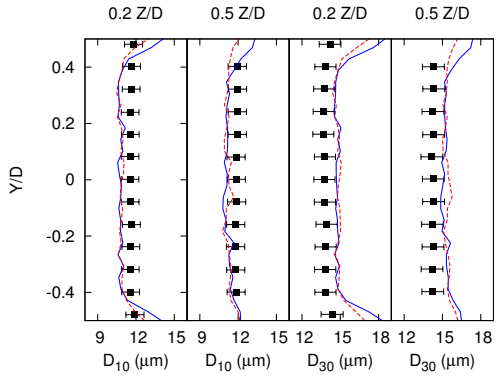


Figure 4. Radial profiles of droplets characteristic diameters $D_{10}$ and $D_{30}$ at two axial positions ( $Z/D = 0.2$ and $Z/D = 0.5$ from the burner exit). Continuous blue line=ATF, dashed red line=$\beta$-PDF and marks=experimental data.

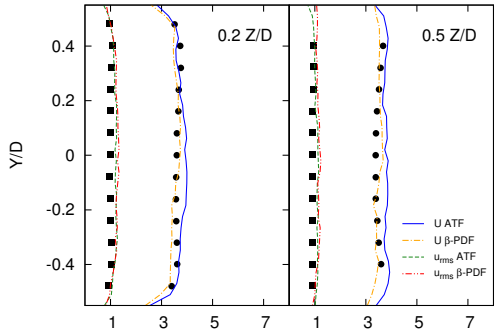


Figure 5. Radial profiles of the mean (U) and fluctuations ($u_{rms}$) of the axial component of droplets velocities at two axial positions ( $Z/D = 0.2$ and $Z/D = 0.5$ from the burner exit).

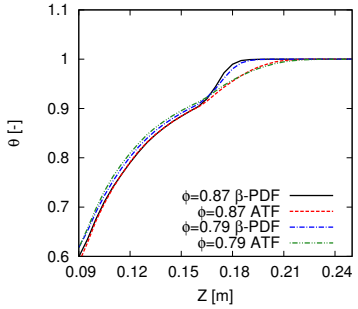


Figure 6. Radial profiles of the mean and fluctuations of the axial component of droplets velocities at two axial positions ( $Z/D = 0.2$ and $Z/D = 0.5$ from the burner exit).

models are clearly evidenced.

Indeed, the tendency on the increase of the flame penetration according to the reduction of the global equivalence ratio is captured by both models. However, this effect is much more pronounced in the ATF modeling. Furthermore, the flame structure predicted with the ATF model agrees fairly well with experimental data, while noticeable discrepancies are observed for the $\beta$-PDF approach.

The shorter flame predicted with the $\beta$-PDF approach induces higher temperatures in the region close to the burner exit, which is reflected in the evaporation degree plots in Fig. 6. In these plots, one can clearly see the sudden increase of the evaporation degree after the burner exit ($Z > 0.16m$) for the $\beta$-PDF approach simulations.

The success of the ATF modeling in these test cases can be understood by the premixed-like flame mode attained with the LPP burner. Undoubtedly, the possibility to solve the flame with the chemical kinetics earned with the flame thickening and the further modeling of the SGS flame wrinkling with the efficiency function attends pretty well the requirements of propagating flames modeling in the flamelet regime. The $\beta$-PDF approach also tends to thicken the reaction zone and is able to predict the flame wrinkling (Vreman *et al.* (2008)). Nevertheless, in this context the stochastic distributions of the control variables should be close to the $\beta$ shape function, which is not always the case for a spray flame (see Ge & Gutheil (2008)). Additionally, the assumption of the statistical independence between the control variables as well as the gradient formulation frequently adopted in LES (Chrigui *et al.* (2012); Sacomano Filho *et al.* (2014); Knudsen & Pitsch (2015); Vreman *et al.* (2008)) also reduces the accuracy of this method.

Certainly, improving the LES resolution the quality of the predicted flame with the presumed PDF approach increases. In this sense, smaller scales of the reacting flow are solved and, consequently, the importance of the role played by the SGS combustion model diminishes. Since this work aims to explore the functionality of combustion models for typical LES, analysis of mesh resolution on the flame zone are not further addressed.

## CONCLUSION

A comparison between two different SGS combustion models, i.e. a presumed PDF and the ATF model, to predict a turbulent spray flame is achieved in the framework of an Eulerian-Lagrangian description. The two approaches are coupled to a tabulated FGM chemistry database built with adiabatic premixed flamelets. The models deliver different structure of the flame and it turns out that the ATF model shows a better agreement with the experimental measurements. The spray characteristics, e.g. droplets diameters and velocities also show good agreement for both models at the investigated positions. It was noticed that the distorted flame structure predicted with the $\beta$-PDF approach also affects the spray characteristics.

From the achieved results, it could be observed that for turbulent spray flames, where the premixed-like combustion mode is present, the usage of the presumed $\beta$-PDF approach shall be done with care. This work could be extended through sensitivity analysis of the parameter $C_{eq}$ (see Eq. 3), and the usage of a dynamic formulation to compute the variances.

## ACKNOWLEDGEMENTS

This work is supported by the German Council of Research (DFG), (SFB/TRR 75). The first author specially acknowledges the financial support (scholarship) by the CNPq (Brazil) and DAAD (Germany).

Despite of this 5K of temperature difference, the data is quite suitable to evaluate the flame structure, according to the low change in the flame speed.

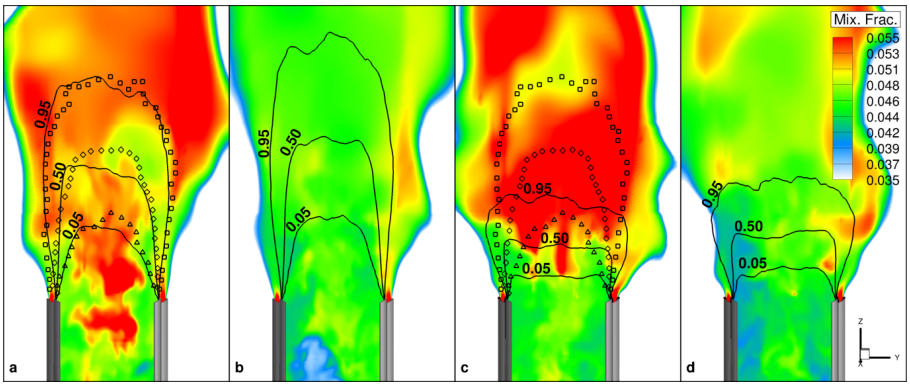


Figure 7. Structure of the four simulated flames colored with instantaneous fields of the mixture fraction. The labeled lines are related to mean values of the progress variable defined in Pichard *et al.* (2002). The corresponding experimental data are represented by marks: $\triangle = 0.05$, $\diamond = 0.50$ and $\square = 0.95$. **a**: flame $\phi = 0.87$ with ATF; **b**: flame $\phi = 0.79$ with ATF; **c**: flame $\phi = 0.87$ with $\beta$-PDF and **d**: flame $\phi = 0.79$ with $\beta$-PDF.

## REFERENCES


Bellan, J. & Harstad, K. 1987 Analysis of the convective evaporation of nondilute clusters of drops. *Int. J. Heat Mass Transfer* **30** (1), 125–136.

Boileau, M., Pascaud, S., Riber, E., Cuenot, B., Gicquel, L. Y. M., Poinsot, T. J. & Cazalens, M. 2008*a* Investigation of Two-Fluid Methods for Large Eddy Simulation of Spray Combustion in Gas Turbines. *Flow Turbul. Combust.* **80** (3), 291–321.

Boileau, M, Staffelbach, G, Cuenot, B, Poinsot, T & Berat, C 2008*b* LES of an ignition sequence in a gas turbine engine. *Combust. Flame* **154** (1-2), 2–22.

Charlette, F., Meneveau, C. & Veynante, D. 2002 A power-law flame wrinkling model for LES of premixed turbulent combustion Part I: non-dynamic formulation and initial tests. *Combust. Flame* **131** (1-2), 159–180.

Chrigui, M., Gounder, J., Sadiki, A., Masri, A. R. & Janicka, J. 2012 Partially premixed reacting acetone spray using LES and FGM tabulated chemistry. *Combust. Flame* **159** (8), 2718–2741.

Chrigui, M., Masri, a. R., Sadiki, a. & Janicka, J. 2013 Large Eddy Simulation of a Polydisperse Ethanol Spray Flame. *Flow Turbul. Combust.* **90** (4), 813–832.

Colin, O., Ducros, F., Veynante, D. & Poinsot, T. 2000 A thickened flame model for large eddy simulations of turbulent premixed combustion. *Phys. Fluids* **12** (7), 1843.

Durand, L. & Polifke, W. 2007 Implementation of the Thickened Flame Model for Large Eddy Simulation of Turbulent Premixed Combustion in a Commercial Solver. *Volume 2: Turbo Expo 2007* pp. 869–878.

Ge, H.-W. & Gutheil, E. 2008 Simulation of a turbulent spray flame using coupled PDF gas phase and spray flamelet modeling. *Combust. Flame* **153** (1-2), 173–185.

Jenny, P., Roekaerts, D. & Beishuizen, N. 2012 Modeling of turbulent dilute spray combustion. *Prog. Energy Combust. Sci.* **38** (6), 846–887.

Jones, W.P., Marquis, A.J. & Noh, D. 2015 LES of a methanol spray flame with a stochastic sub-grid model. *Proc. Combust. Inst.* **35** (2), 1685–1691.

Knudsen, E. & Pitsch, H. 2015 Modeling partially premixed combustion behavior in multiphase LES. *Combust. Flame* **162** (1), 159–180.

Kuenne, G., Seffrin, F., Fuest, F., Stahler, T., Ketelheun, A., Geyer, D., Janicka, J. & Dreizler, A. 2012 Experimental and numerical analysis of a lean premixed stratified burner using 1D Raman/Rayleigh scattering and large eddy simulation. *Combust. Flame* **159** (8), 2669–2689.

Meneveau, C. & Poinsot, T. 1991 Stretching and quenching of flamelets in premixed turbulent combustion. *Combust. Flame* **86** (4), 311–332.

Miller, R. S., Harstad, K. & Bellan, J. 1998 Evaluation of equilibrium and non-equilibrium evaporation models for many-droplet gas-liquid ow simulations. *Int. J. Multiphase Flow* **24**, 1025–1055.

Oijen, J. A. van 2015 CHEM1D.

O'Rourke, P. J. & Bracco, F. V: 1979 Two scaling transformations for the numerical computation of multidimensional unsteady laminar flames. *J. Comput. Phys.* **33** (2), 185–203.

Pichard, C. 2003 Caractérisation expérimentale de l ' atomisation et de la combustion d ' un mélange diphasique partiellement prévaporisé et prémélangé. PhD thesis, Universite D'Orleans.

Pichard, C., Michou, Y., Chauveau, C. & Gökalp, L. 2002 Average droplet vaporization rates in partially prevaporized turbulent spray flames. *Proc. Combust. Inst.* **29** (1), 527–533.

Poinsot, T. & Veynante, D. 2012 *Theoretical and Numerical Combustion*.

Prasad, V. N., Masri, A. R., Navarro-Martinez, S. & Luo, Kai H. 2013 Investigation of auto-ignition in turbulent methanol spray flames using Large Eddy Simulation. *Combust. Flame* **160** (12), 2941–2954.

Reveillon, J. & Vervisch, L. 2005 Analysis of weakly turbulent dilute-spray flames and spray combustion regimes. *J. Fluid. Mech.* **537** (-1), 317.

Sacomano Filho, F. L., Chrigui, M., Sadiki, A. & Janicka, J. 2014 Les-Based Numerical Analysis of Droplet Vaporization Process in Lean Partially Premixed Turbulent Spray Flames. *Combust. Sci. Technol.* **186** (4-5), 435–452.

Vreman, A., Albrecht, B., Vanoijen, J., Degoey, L. & Bastiaans, R. 2008 Premixed and nonpremixed generated manifolds in large-eddy simulation of Sandia flame D and F. *Combust. Flame* **153** (3), 394–416.

Yoo, C. S., Lu, T., Chen, J. H. & Law, C. K. 2011 Direct numerical simulations of ignition of a lean n-heptane/air mixture with temperature inhomogeneities at constant volume: Parametric study. *Combust. Flame* **158** (9), 1727–1741.